Priority Report

Cancer Research

Mechanistic Rationale to Target PTEN-Deficient Tumor Cells with Inhibitors of the DNA Damage Response Kinase ATM

Nuala McCabe[1,2], Conor Hanna[1], Steven M. Walker[1,2], David Gonda[3], Jie Li[3], Katarina Wikstrom[2], Kienan I. Savage[1], Karl T. Butterworth[1], Clark Chen[3], D. Paul Harkin[1,2], Kevin M. Prise[1], and Richard D. Kennedy[1,2]

Abstract

Ataxia telangiectasia mutated (ATM) is an important signaling molecule in the DNA damage response (DDR). ATM loss of function can produce a synthetic lethal phenotype in combination with tumor-associated mutations in FA/BRCA pathway components. In this study, we took an siRNA screening strategy to identify other tumor suppressors that, when inhibited, similarly sensitized cells to ATM inhibition. In this manner, we determined that PTEN and ATM were synthetically lethal when jointly inhibited. PTEN-deficient cells exhibited elevated levels of reactive oxygen species, increased endogenous DNA damage, and constitutive ATM activation. ATM inhibition caused catastrophic DNA damage, mitotic cell cycle arrest, and apoptosis specifically in PTEN-deficient cells in comparison with wild-type cells. Antioxidants abrogated the increase in DNA damage and ATM activation in PTEN-deficient cells, suggesting a requirement for oxidative DNA damage in the mechanism of cell death. Lastly, the ATM inhibitor KU-60019 was specifically toxic to PTEN mutant cancer cells in tumor xenografts and reversible by reintroduction of wild-type PTEN. Together, our results offer a mechanistic rationale for clinical evaluation of ATM inhibitors in PTEN-deficient tumors. *Cancer Res; 75(11); 2159–65. ©2015 AACR.*

Introduction

Ataxia telangiectasia mutated (ATM) is the primary kinase that responds to DNA double-strand breaks (DSB; ref. 1). Therapeutic inhibition of ATM has been shown to sensitize cells to ionizing radiation and DNA-damaging chemotherapeutic agents (2, 3), suggesting that it may have a role in combination therapy for cancer. Increasingly, however, it has been found that DNA damage response–targeted therapies, for example PARP inhibitors, may also exhibit single-agent activity in the context of loss of specific tumor suppressors, such as BRCA1 or BRCA2 (4) ATM inhibitors have a potential role as single agents in the context of loss of components of the FA/BRCA pathway (5). An siRNA library screen identified synthetic lethality between loss of ATM function and loss of various components of the FA/BRCA pathway that have been reported in human cancers. Combined loss of ATM and the FA/BRCA pathway resulted in the accumulation of lethal DNA damage and cell death. In the current study, we ask if loss of ATM could be synthetically lethal with other known human tumor suppressors, thereby indicating other single-agent targets for ATM inhibitors. We use an siRNA library designed to individually target known human tumor suppressors to screen against an isogenic ATM wild-type and deficient cell line system in order to identify synthetic lethal interactions. We consequently identify synthetic lethality between PTEN and ATM and demonstrate a role for ATM in promoting the survival of PTEN-deficient cells through the signaling of oxidative DNA damage.

Materials and Methods

Cell lines

All cell lines were sourced from the ATCC. HCT116 cells lacking wild-type PTEN have been described previously and were licensed from Georgetown University (6). The PC3-PTEN–inducible cell lines (7) and ATM-deficient human fibroblasts and reconstituted cells have previously been described (Supplementary Information; and Supplementary Fig. S1A; ref. 8).

Cell cycle, apoptosis, and mitotic chromosome analysis

Cells were fixed in 70% ethanol, incubated with RNase A and propidium iodide (PI), and analyzed with a FACSCalibur (Becton Dickinson) using CellQuest Pro software. For phospho-histone H3 analysis, cells were incubated with anti–phospho-histone H3 antibody (Upstate Biotechnology). Apoptotic assays were performed using the luminescence Caspase-Glo 3/7 assay from Promega. To assess chromosome damage, cells were treated with colcemid (0.05 μg/mL; KaryoMAX; GibcoBRL) for 4 hours.

[1]Centre for Cancer Research and Cell Biology, Queens University Belfast, Northern Ireland, United Kingdom. [2]Almac Diagnostics, Craigavon, Northern Ireland, United Kingdom. [3]University of California, San Diego, La Jolla, California.

Note: Supplementary data for this article are available at Cancer Research Online (http://cancerres.aacrjournals.org/).

N. McCabe and C. Hanna contributed equally to this article.

Corresponding Authors: Richard D. Kennedy, Queens University Belfast, CCRCB, 97 Lisburn Road, Belfast, Northern Ireland BT9 7BL, UK. Phone: 44-0-28-9097-2760; Fax: 44-0-28-9097-2776; E-mail: r.kennedy@qub.ac.uk; or Kevin M. Prise, k.prise@qub.ac.uk

doi: 10.1158/0008-5472.CAN-14-3502

Western blotting analysis

Cell pellets were lysed in 20 mmol/L Tris (pH 8), 200 mmol/L NaCl, 1 mmol/L EDTA, 0.5% (v/v) NP-40, and 10% (v/v) glycerol. For phospho-H2AX detection, histones were extracted overnight at 4°C in 0.2N HCL from protein pellets. Lysates and histone extracts were electrophoresed on NuPage precast gels (Invitrogen), and immunoblotted with anti–phospho-H2AX (Cell Signaling Technology), anti-PTEN (Santa Cruz), anti–phospho-ATM ser1981 (Cell Signaling Technology), anti–phospho-CHK2 thr68 (Cell Signaling Technology), and anti–phospho-AKT ser473 (Cell Signaling Technology). As loading controls, anti–β-Actin (Sigma), anti–vinculin (Cell Signaling Technology), and anti-Tubulin (Abcam) were used. This was followed by incubation with anti–IgG-HRP (Cell Signaling Technology) and chemiluminescent detection (ECL-PLUS).

Reactive oxygen species detection

Cells were incubated with 5 μmol/L CM-H_2DCF-DA (Invitrogen) for 30 minutes followed by flow cytometry.

Colony formation assays

Cells were seeded at predetermined densities, 24 hours later treated with KU-55933 (Calbiochem), which was replenished every 3 to 4 days. Where appropriate, cells were transfected with gene-specific targeting siRNAs (Qiagen) using Lipofectamine RNAiMAX (Invitrogen), and 48 hours later counted and seeded for colony formation assay. After 10 days, cells were washed with PBS, fixed in methanol, stained with crystal violet, and colonies counted. The surviving fraction for a given dose/siRNA was calculated, and dose–response curves were plotted using GraphPad Prism 5 (*, $P \leq 0.05$, Student t test).

siRNA screening

A customized siRNA library targeting 178 tumor suppressor genes or genes whose loss of function was associated with cancer (Supplementary Table S1) was developed using predesigned siRNA sequences (Qiagen). The library contained 3 independent siRNA sequences per gene and was provided in an arrayed format in 96-well plates. ATM-deficient and ATM-complemented cells were reverse transfected with the siRNA library (Qiagen) using Lipofectamine RNAiMax reagent (Life Technologies; Supplementary Information).

Xenograft study

Cells (3×10^7) were implanted into male Fox Chase Severe Combined Immunodeficiency (SCID) mice (Charles River Laboratories). Administration of doxycycline was started when tumors reached 100 mm^3 in volume and was performed every 48 hours up to removal of the animal from the experiment. Forty-eight hours after PTEN induction, animals were administered KU-60019 (100 mg/kg) for 5 consecutive days and measured until they reached a target 400 mm^3 volume. Measurements of tumor volume and body weight took place every 3 days using calipers (Supplementary Information).

Results

ATM is a potential drug target for PTEN-deficient cells

In order to identify potential synthetic lethality interactions with ATM loss, we used a customized siRNA library targeting 178 tumor suppressor genes (Supplementary Table S1). The library was used to screen against ATM-deficient and ATM-complemented fibroblasts (Supplementary Fig. S1A; ref. 8). This isogenic cell line was found to be preferable to therapeutic ATM inhibition for the purpose of initial screening as there was less likely to be nonspecific off-target interactions with the siRNA targets or the ATP-dependent reagents used for viability read-out. Robust Z-scores were calculated for three independent siRNA per gene, and an average value was then generated. The screen identified 9 genes that were synthetically lethal with loss of PTEN (Table 1). Each of these nine genes demonstrated an average Robust Z-score ≤ -2 (Fig. 1A). Consistent with previous data, we found that components of the FA/BRCA pathway were synthetically lethal with ATM loss. In addition, CDKN2C and p53 genes involved in the G_1–S checkpoint were synthetically lethal with ATM deficiency, indicating that they may play a compensatory role in maintaining cellular viability in the absence of ATM-mediated cell cycle check pointing. Interestingly, the tumor suppressor PTEN was also synthetically lethal with ATM. Similar to ATM, PTEN had been reported to have a direct role in the DNA damage response (9–11), and loss of its function represents a potentially important drug target, as inactivating mutations are associated with incurable cancers such as advanced prostate cancer and glioblastoma (12). We therefore took PTEN forward into secondary validation as a synthetic lethal candidate.

For validation of PTEN as a hit from the screen, we performed colony formation assays in the ATM isogenic cells. PTEN knockdown using two independent siRNAs resulted in reduced survival of ATM-deficient cells compared with ATM wild-type corrected cells (fold difference of 48% and 40%; Fig.1B). Next, we assessed the sensitivity of the HCT116 (6) and PC3 (7) isogenic cell line models (Supplementary Fig. S1A and S1B) to loss of ATM function using either gene-specific siRNA or the ATM inhibitor KU-55933 (2). Both the PTEN-deficient cell lines demonstrated increased sensitivity to siRNA-mediated knockdown of ATM (fold difference of 20% and 42%; Fig. 1C) and increased sensitivity to the KU-55933 (fold change in IC_{50} of 16 and 8) compared with wild-type counterparts (Fig. 1D). PTEN-null cells have constitutive activation of AKT. We therefore ensured that KU-55933 did not inhibit AKT, and the observed sensitivity in PTEN-null cells was independent of AKT function (Supplementary Fig. S2).

To confirm that the observed ATM inhibitor sensitivity in PTEN-deficient cells was not model specific, we tested a panel of cell lines representing PTEN wild-type and -deficient states in prostate cancer, glioblastoma, breast cancer, and normal cells.

Table 1. siRNA hits

Gene	Function	Average Z score
BRIP1 (FANCJ)	DNA repair	−10.029
CDKN2C	G_1–S checkpoint	−8.373
PTEN	Negative regulator PI3K	−6.256
STEAP4	Immunity and response to oxidative stress	−5.322
NKTR	Immunity	−4.452
CASP8	Apoptosis	−2.541
TP53	G_1–S checkpoint	−2.459
FANCG	DNA repair	−2.316
CAV1	Cell cycle progression/ RAS signaling	−2.023

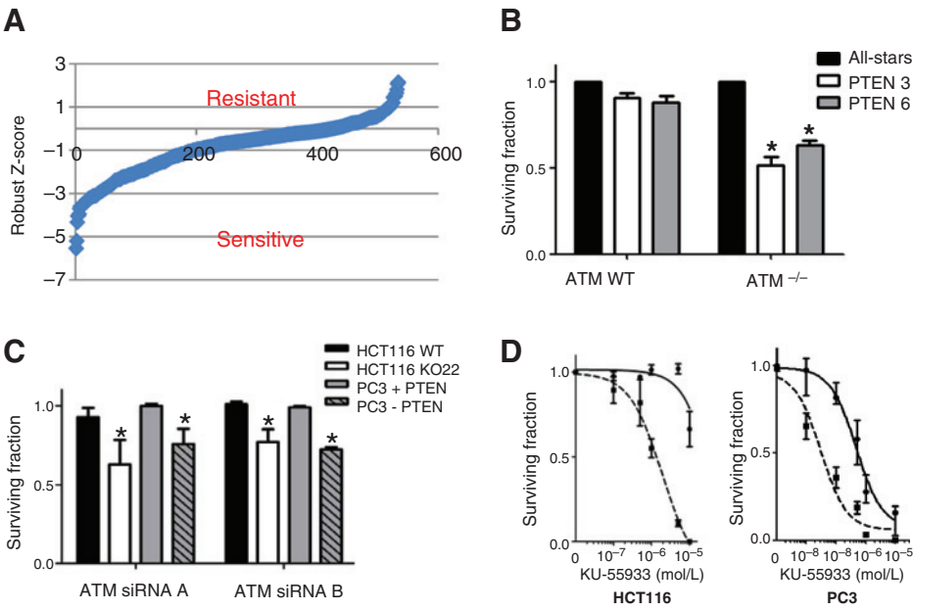

Figure 1.
ATM is a potential drug target for PTEN-deficient cells. A, robust Z score distribution of siRNAs targeting 178 tumor suppressor genes in ATM isogenic cell line models. B, colony formation assay demonstrating synthetic lethality in the ATM fibroblast isogenic model system transfected with two independent siRNAs specifically targeting PTEN (Qiagen). Survival fractions were calculated based on scrambled control, transfected cells (*, $P \leq 0.05$, Student *t* test; validation of the siRNA targeting PTEN, Supplementary Fig. S1B). C, colony formation assay demonstrating synthetic lethality in the HCT116 and PC3 PTEN isogenic model systems transfected with two siRNAs specifically targeting ATM (Qiagen; validation of the siRNA targeting ATM; Supplementary Fig. S1B; *, $P \leq 0.05$, Student *t* test). PTEN wild-type cells: HCT WT and PC3+PTEN and PTEN-deficient cells, HCT KO22 and PC3-PTEN. D, colony formation assay demonstrating synthetic lethality in the HCT116 and PC3 PTEN isogenic model systems treated with increasing concentrations of the ATM inhibitor KU-55933. Survival fractions were calculated based on DMSO-treated cells. Solid lines, PTEN wild-type cells; broken lines, PTEN-deficient cells.

In each case, the PTEN-deficient cell line demonstrated increased sensitivity to the ATM inhibitor KU-55933 compared with the PTEN wild-type cell line (Supplementary Fig. S1C), suggesting that this strategy may be of value as a treatment in more than one cancer type. In addition, advanced prostate cancers and glioblastomas are associated with PTEN loss (12) and are often treated with radiation; hence, ATM inhibitors may be particularly useful in these indications where they may have a dual role.

PTEN-deficient cells have elevated levels of ROS, DNA damage, and activation of ATM

It has previously been reported that PTEN-deficient cells exhibit abnormal homologous recombination (HR)–mediated DNA repair through loss of expression of RAD51 (9, 13). However, this observation has not been consistent across cell line models (10–11) or in human tumor samples (14). Loss of RAD51 expression could potentially have accounted for the synthetic lethal interaction between PTEN and ATM. However, we did not find any association between RAD51 expression or foci formation and PTEN expression in our isogenic cell line systems with or without DNA damage, suggesting that HR functions normally in both cell lines (Supplementary Fig. S3A and S3B). Moreover, both PTEN wild-type and -deficient cells were sensitive to depletion of RAD51 by siRNA, the sensitivity being more pronounced in the deficient cells (Supplementary Fig. S3C). This further supports an alternative mechanism to loss of HR in PTEN-deficient cells underlying the synthetic lethality with ATM inhibition.

PTEN-null mouse embryonic fibroblasts have been reported to exhibit increased oxidative DNA damage (15), we therefore asked if there were increased levels of oxidative damage in the PC3 and HCT116 isogenic models. We used a fluorescence-based assay to measure reactive oxygen species (ROS) and observed a shift in the fluorescence intensity of 10±1% and 12±2% associated with PTEN deficiency in HCT116 and PC3 isogenic cell line models, respectively (Fig. 2A). In addition, there was a greater induction of ROS in PTEN-deficient compared with wild-type cells in the presence of the KU-55933 with increases of 21±2% and 25±3% in HCT116 and PC3, respectively. This observation suggests that ATM inhibition may further enhance oxidative stress in PTEN-null cells. Oxidative DNA lesions have been reported to result in DSBs with consequent induction of histone-H2AX phosphorylation (γ-H2AX), a marker of DSBs (16). Consistent with this, the PTEN-deficient cell lines demonstrated increased baseline levels of γ-H2AX (Fig. 2B and Supplementary Fig. S3D). In addition, Western blot analysis demonstrated constitutive phosphorylation of ATM (a marker of activation) and its substrate Chk2, in PTEN-deficient cells (Fig. 2B), consistent with an ATM-mediated response to DSBs.

To further investigate if the observed increase in γ-H2AX and ATM phosphorylation in PTEN-deficient cells was the result of increased oxidative damage, we pretreated the PTEN-deficient cell line HCT116 KO22 with the antioxidants N-acetyl cysteine or beta-carotene. Following treatment with these agents, we observed reduced γ-H2AX expression and

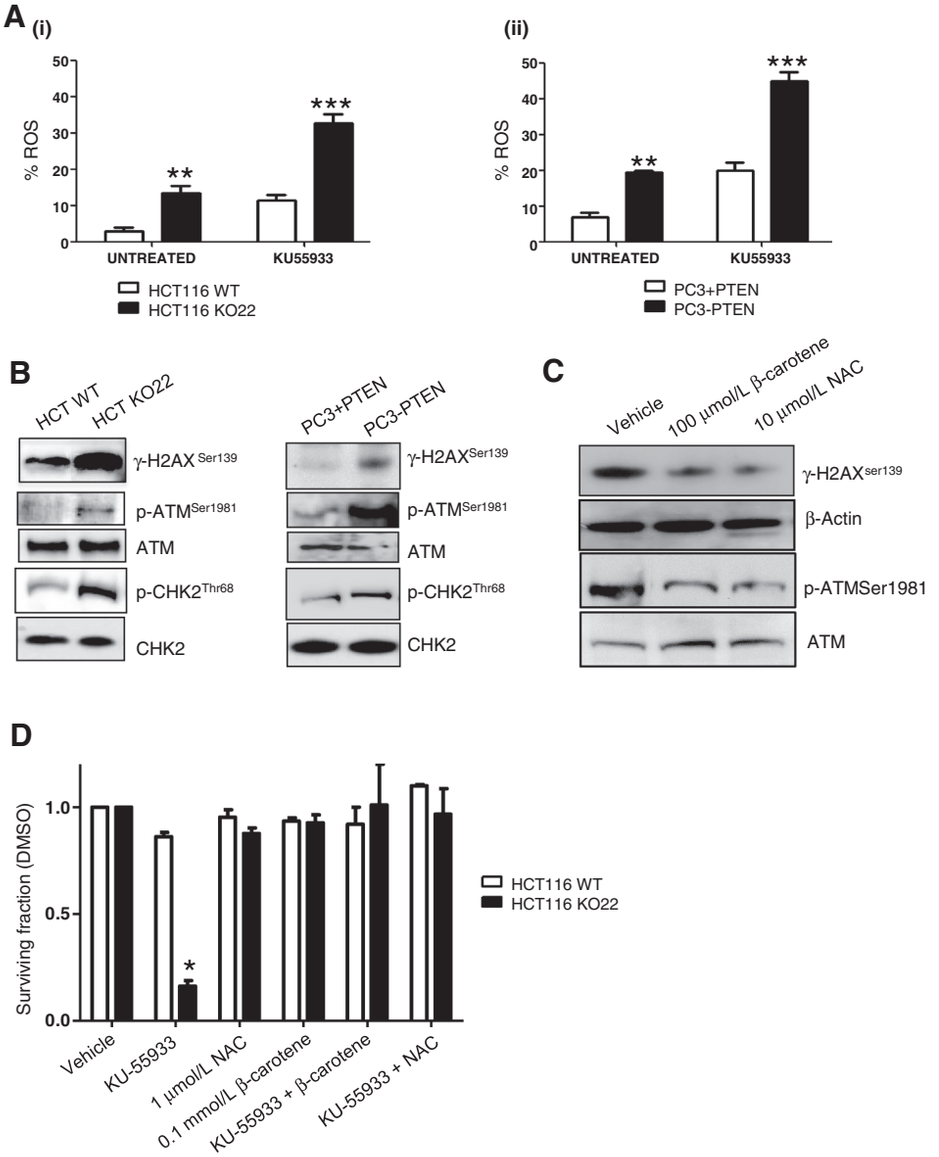

Figure 2.
PTEN-deficient cells have elevated levels of ROS, DNA damage, and activation of ATM. A, oxidative stress assay demonstrating increased basal ROS in HCT116 (i) and PC3 PTEN (ii) isogenic cells. **, $P \leq 0.01$; ***, $P \leq 0.001$, Student *t* test. B, increased γ-H2AX, phospho-ATM serine 1981, and phospho-CHK2 threonine 68 levels in PTEN HCT116 (KO22) and PC3 (PC3-PTEN) deficient cells compared with wild-type counterparts. Total ATM and CHK2 were used as loading controls. C, reversal of increased γ-H2AX and phospho-ATM levels in PTEN-deficient HCT116 and PC3 cells treated with 100 μmol/L β-carotene or 10 μmol/L NAC. β-Actin and total ATM were used as loading controls. D, colony formation assay of PTEN wild-type and -deficient HCT116 cells treated with 10 μmol/L KU-55933 in the absence and presence of 100 μmol/L β-carotene or 10 μmol/L NAC. *, $P \leq 0.05$, Student *t* test.

phospho-ATM, indicating that oxidative DNA damage was the likely cause for the increase in DSBs (Fig. 2C). In summary, these data suggest that PTEN-deficient cells have high levels of oxidative stress, resulting in increased DNA damage and subsequent ATM activation.

Next, we asked if the observed increase in oxidative DNA damage in PTEN-deficient cells was required for ATM inhibitor sensitivity. We pretreated the HCT116 PTEN-deficient and wild-type isogenic cell lines with N-acetyl cysteine or beta-carotene and tested the sensitivity to the ATM inhibitor KU-55933 (Fig. 2D). Each of the antioxidants rescued KU-55933 sensitivity in the PTEN-deficient cell line, indicating that oxidative damage is required to sensitize PTEN-deficient cells to ATM inhibition.

Acute inhibition of ATM in PTEN-deficient cells results in cell cycle arrest, chromosome aberrations, and apoptosis

To investigate how DNA damage following ATM inhibition resulted in a loss of cellular viability specifically in PTEN-deficient cells, we analyzed the cell cycle profile of the cells with or without KU-55933 treatment. ATM inhibition resulted in a greater G_2–M arrest in the HCT116 PTEN-deficient cells compared with wild-type cells (Fig. 3A). Furthermore, analysis of Histone H3 serine 10 phosphorylation (a measure of the mitotic cellular population) demonstrated that these cells were specifically arrested in mitosis (Fig. 3B). We then examined whether the accumulation of cells in M phase was associated with DNA damage. Chromosome spreads demonstrated an increase in aberrations, predominantly in the PTEN-deficient cells, including radial chromosomes following ATM inhibition (Fig. 3C). This indicates that in PTEN-deficient cells, ATM normally functions to prevent catastrophic DNA damage progressing into the M phase of the cell cycle. Furthermore, treatment with the ATM inhibitor resulted in increased caspase 3/7 activation specifically in the HCT116 PTEN-deficient cell line (62%) compared with wild-type counterpart (8%) consistent with apoptotic cell death (Fig. 3D).

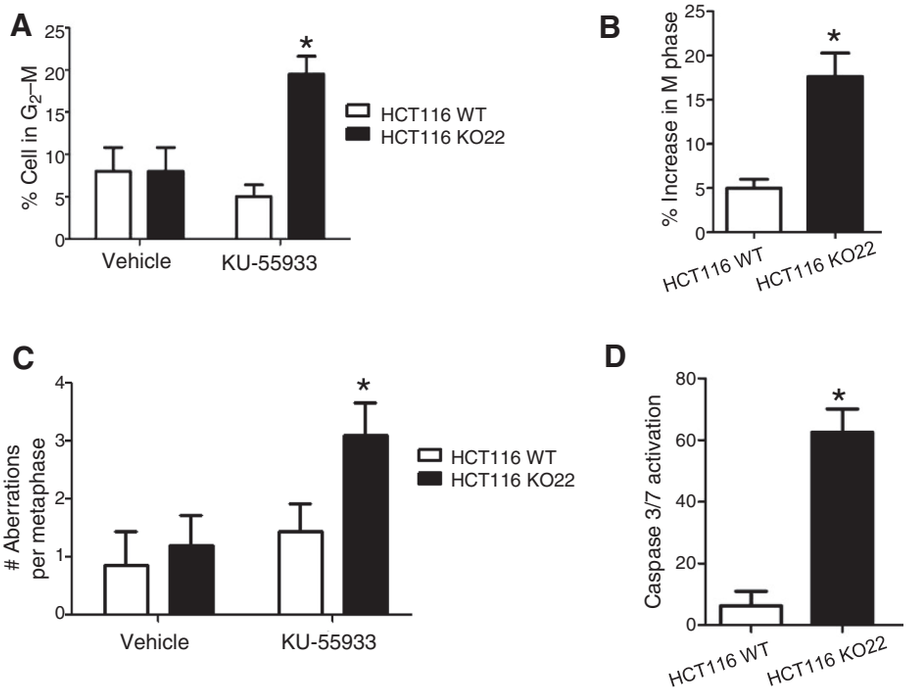

Figure 3.
Acute inhibition of ATM in PTEN-null cells results in cell cycle arrest, chromosome aberrations, and apoptosis. A, G_2–M arrest in PTEN-deficient HCT116 cells treated with 10 μmol/L KU-55933 for 72 hours (*, $P \leq 0.05$). B, M phase arrest in PTEN-deficient HCT116 cells treated with 10 μmol/L KU-55933 for 72 hours (*, $P \leq 0.05$). Percent increase from DMSO-treated cells. C, increased chromosome breaks and aberrations in PTEN-deficient HCT116 cells after treatment with 10 μmol/L KU-55933 for 72 hours (*, $P \leq 0.05$). D, HCT116 wild-type and KO22 cells were treated with 10 μmol/L KU-55933 for 96 hours and analyzed for caspase 3/7 activation (*, $P \leq 0.05$). Percent increase from DMSO-treated cells.

In vivo efficacy of ATM inhibition in PTEN-deficient xenografts

To investigate the *in vivo* efficacy of ATM-specific inhibition in PTEN-deficient cells, we used the PC3 PTEN tetracycline–inducible cell line model in a subcutaneous xenograft setting. Firstly, we established that the Tetracycline derivative doxycycline was efficient at inducing PTEN expression *in vitro* (Supplementary Fig. S4A) and *in vivo* (Supplementary Fig. S4B).

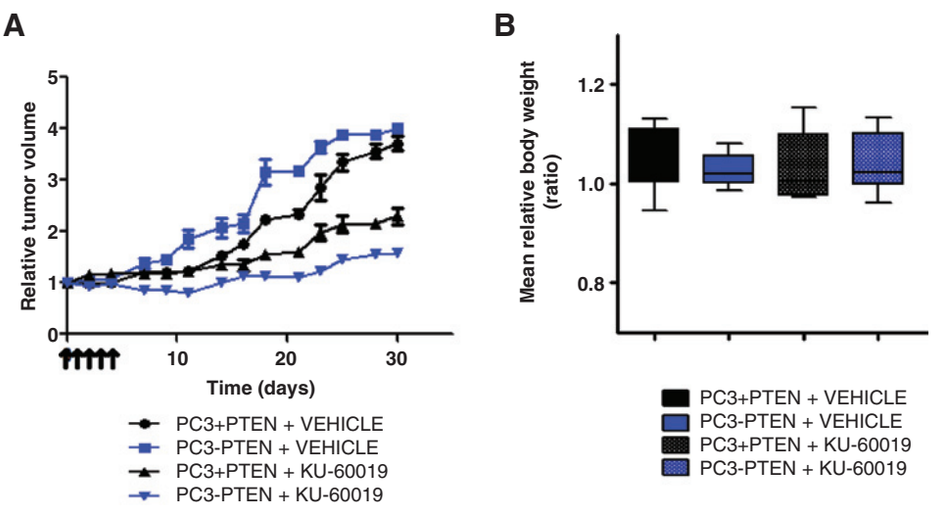

Figure 4.
In vivo efficacy of ATM inhibition in PTEN-deficient xenografts. A, relative tumor volume curves for $PTEN^{+/+}$ untreated control (●), $PTEN^{-/-}$ untreated control (●), KU-60019–treated $PTEN^{+/+}$ (■) and $PTEN^{-/-}$ (■) PC-3 xenografts. Mean relative tumor volume is plotted against time from initial treatment. Target tumor volume was 400 mm^3, i.e., 4-fold increase in size from initial treatment. The *t* tests were performed at 30 days. Each treatment group contained four animals. B, box plot of mean relative change in body weight during treatments.

COMPARISON	T-Test
PTEN WT VS. DEFICIENT (VEHICLE)	0.3218
PTEN WT VEHICLE VS. PTEN WT KU60019	0.1213
PTEN DEFICIENT VEHICLE VS. KU60019	0.0004
PTEN WT VS. PTEN DEFICIENT (KU60019)	0.006

Calliper measurements of tumor volumes showed that induction of PTEN using doxycycline led to a slowing of tumor growth from 72 hours onwards (Supplementary Fig. S4C). Next, we investigated the selective toxicity of the ATM-specific kinase inhibitor KU-60019 (17) as a single modality in the PC3-PTEN–inducible model. This inhibitor was chosen, as it is a potent ATM inhibitor and unlike KU-55933 is active in animal systems. Despite PTEN-deficient control tumors reaching a 4-fold increase in size before PTEN wild-type controls, KU-60019–treated PTEN-deficient tumors displayed a statistically significant slowing in growth (Fig. 4A). This growth inhibition was especially evident at the start of the experiment (days 5–12) just after KU-60019 was administered (days 1–5). There were no significant changes in the mean relative body weights of each treatment groups (Fig. 4B). Inducible PTEN expression *in vivo* was analyzed in resected tumors by immunofluorescence (Supplementary Fig. S4D).

Discussion

PTEN lost in a wide variety of human cancers (12), and its primary role as a tumor suppressor is through inhibition of the PI3/AKT pathway (18). However more recently, PTEN has been reported to maintain genomic integrity and confer resistance to ionizing radiation and PARP inhibition (9–11, 13), which is a nuclear function and independent from AKT regulation (19). In the current study, we have reported a synthetic lethal interaction between loss of ATM and loss of PTEN. Loss of PTEN results in increased oxidative damage, which is required for the sensitization to ATM inhibition, as antioxidants can rescue PTEN-deficient cells from ATM inhibitor–mediated cell death. Oxidative DNA lesions can result in stalled DNA replication forks and resultant DSBs (16) and activation of ATM (1). Hence, loss of ATM function in PTEN-deficient cells may therefore result in a persistence of oxidative DNA lesions and inactivation of the G_2–M checkpoint, allowing cells with catastrophic DNA damage to enter the M phase of the cell cycle and undergo cell death. Importantly, ATM has been reported to function to prevent malignant progression of premalignant conditions through the signaling of oncogene-related DNA damage (20). Our data suggest that once a cell has become malignant through additional genetic abnormalities, e.g., loss of PTEN, the cancer cell can then become dependent on ATM activation to maintain a level of DNA integrity required for survival. In summary, we have demonstrated that PTEN and ATM are synthetically lethal, and, furthermore, we have found a requirement for ATM in the maintenance of DNA integrity and cellular viability in the presence of increased oxidative damage secondary to PTEN deficiency. The selective sensitivity of PTEN-deficient tumors to ATM inhibition *in vivo* suggests that this may represent a novel approach to targeted cancer therapy in the clinic.

Disclosure of Potential Conflicts of Interest

No potential conflicts of interest were disclosed.

Authors' Contributions

Conception and design: N. McCabe, J. Li, C. Chen, D.P. Harkin, K.M. Prise, R.D. Kennedy

Development of methodology: N. McCabe, C. Hanna, K. Wikstrom, K.T. Butterworth, R.D. Kennedy

Acquisition of data (provided animals, acquired and managed patients, provided facilities, etc.): N. McCabe, C. Hanna, S.M. Walker, K. Wikstrom, K.I. Savage, K.T. Butterworth, C. Chen, R.D. Kennedy

Analysis and interpretation of data (e.g., statistical analysis, biostatistics, computational analysis): N. McCabe, C. Hanna, S.M. Walker, D. Gonda, J. Li, K.I. Savage, C. Chen, K.M. Prise, R.D. Kennedy

Writing, review, and/or revision of the manuscript: N. McCabe, S.M. Walker, K.I. Savage, C. Chen, D.P. Harkin, K.M. Prise, R.D. Kennedy

Administrative, technical, or material support (i.e., reporting or organizing data, constructing databases): N. McCabe, J. Li

Study supervision: N. McCabe, D.P. Harkin, K.M. Prise, R.D. Kennedy

Acknowledgments

The authors thank Professor T. Waldman for the HCT116 PTEN isogenic cell line model.

Grant Support

This work was supported by Invest NI (reference ST263) through the European Sustainable Competitiveness Programme 2007–2013, European Regional Development Fund (ERDF), and grants S10-08 from Prostate Cancer UK and CE013_2-004: FASTMAN Centre, Movember Prostate Cancer Centre of Excellence.

Received December 10, 2014; revised March 4, 2015; accepted March 24, 2015; published OnlineFirst April 13, 2015.

References

1. Shiloh Y, Ziv Y. The ATM protein kinase: regulating the cellular response to genotoxic stress, and more. Nat Rev Mol Cell Biol 2013;14:197–210.
2. Hickson I, Zhao Y, Richardson CJ, Green SJ, Martin NM, Orr AI, et al. Identification and characterization of a novel and specific inhibitor of the ataxia-telangiectasia mutated kinase ATM. Cancer Res 2004;64:9152–59.
3. Batey MA, Zhao Y, Kyle S, Richardson C, Slade A, Martin NM, et al. Preclinical evaluation of a novel ATM inhibitor, KU59403, in vitro and in vivo in p53 functional and dysfunctional models of human cancer. Mol Cancer Ther 2013;12:959–67.
4. Lord CJ, Ashworth A. Targeted therapy for cancer using PARP inhibitors. Curr Opin Pharmacol 2008;8:363–9.
5. Kennedy RD, Chen CC, Stuckert P, Archila EM, De la Vega MA, Moreau LA, et al. Fanconi anemia pathway-deficient tumor cells are hypersensitive to inhibition of ataxia telangiectasia mutated. J Clin Invest 2007;117:1440–9.
6. Lee C, Kim JS, Waldman T. PTEN gene targeting reveals a radiation-induced size checkpoint in human cancer cells. Cancer Res 2004;64:6906–14.
7. Maxwell PJ, Coulter J, Walker SM, McKechnie M, Neisen J, McCabe N, et al. Potentiation of inflammatory CXCL8 signaling sustains cell survival in *PTEN*-deficient prostate carcinoma. Eur Urol 2013;64:177–88.
8. Ziv Y, Bar-Shira A, Pecker I, Russell P, Jorgensen TJ, Tsarfati I, et al. Recombinant ATM protein complements the cellular A-T phenotype. Oncogene 1997;15:159–67.
9. Shen WH, Balajee AS, Wang J, Wu H, Eng C, Pandolfi PP, et al. Essential role for nuclear PTEN in maintaining chromosomal integrity. Cell 2007;128:157–70.
10. Gupta A, Yang Q, Pandita RK, Hunt CR, Xiang T, Misri S, et al. Cell cycle checkpoint defects contribute to genomic instability in PTEN-deficient cells independent of DNA DSB repair. Cell Cycle 2009;8:2198–210.
11. McEllin B, Camacho CV, Mukherjee B, Hahm B, Tomimatsu N, Bachoo RM, et al. PTEN loss compromises homologous recombination repair in astrocytes: implications for glioblastoma therapy with temozolomide or poly(ADP-ribose) polymerase inhibitors. Cancer Res 2010;70:5457–64.

12. Li J, Yen C, Liaw D, Podsypanina K, Bose S, Wang SI, et al. PTEN, a putative protein tyrosine phosphatase gene mutated in human brain, breast, and prostate cancer. Science 1997;275:1943–47.
13. Mendes-Pereira AM, Martin SA, Brough R, McCarthy A, Taylor JR, Kim JS, et al. Synthetic lethal targeting of PTEN mutant cells with PARP inhibitors. EMBO Mol Med 2009;1:315–22.
14. Fraser M, Zhao H, Luoto KR, Lundin C, Coackley CL, Chan N, et al. PTEN deletion in prostate cancer cells does not associate with loss of RAD51 function: implications for radiotherapy and chemotherapy. Clin Cancer Res 2012;18:1025–27.
15. Huo YY, Li G, Duan RF, Gou Q, Fu CL, Hu YC, et al. PTEN deletion leads to deregulation of antioxidants and increased oxidative damage in mouse embryonic fibroblasts. Free Radic Biol Med 2008;44: 1578–91.
16. Harper JV, Anderson JA, O'Neill P. Radiation induced DNA DSBs: Contribution from stalled replication forks? DNA Repair 2010;9:907–13.
17. Golding SE, Rosenberg E, Valerie N, Hussaini I, Frigerio M, Cockcroft XF, et al. Improved ATM kinase inhibitor KU-60019 radiosensitizes glioma cells, compromises insulin, AKT and ERK prosurvival signaling, and inhibits migration and invasion. Mol Cancer Ther 2009;8:2894–902.
18. Manning BD, Cantley LC. AKT/PKB signaling: navigating downstream. Cell 2007;129:1261–74.
19. Bassi C, Ho J, Srikumar T, Dowling RJ, Gorrini C, Miller SJ, et al. Nuclear PTEN controls DNA repair and sensitivity to genotoxic stress. Science 2013;341:395–9.
20. Bartkova J, Rezaei N, Liontos M, Karakaidos P, Kletsas D, Issaeva N, et al. Oncogene-induced senescence is part of the tumorigenesis barrier imposed by DNA damage checkpoints. Nature 2006;444:633–7.